Cancer Chemother Pharmacol (2012) 69:71–83
DOI 10.1007/s00280-011-1677-x

ORIGINAL ARTICLE

The marine sponge toxin agelasine B increases the intracellular Ca^{2+} concentration and induces apoptosis in human breast cancer cells (MCF-7)

Adriana A. Pimentel · Pimali Felibertt · Felipe Sojo · Laura Colman · Adriana Mayora · May Li Silva · Hector Rojas · Reinaldo Dipolo · Alírica I. Suarez · Reinaldo S. Compagnone · Francisco Arvelo · Ivan Galindo-Castro · Juan B. De Sanctis · Perla Chirino · Gustavo Benaim

Received: 6 March 2011 / Accepted: 9 May 2011 / Published online: 21 May 2011

Abstract
Purpose In search for new drugs derived from natural products for the possible treatment of cancer, we studied the action of agelasine B, a compound purified from a marine sponge *Agelas clathrodes*.
Methods Agelasine B was purified from a marine sponge *Agelas clathrodes* and assayed for cytotoxicity by MTT on two human breast cancer cells (MCF-7 and SKBr3), on a prostate cancer cells (PC-3) and on human fibroblasts. Changes in the intracellular Ca^{2+} concentrations were assessed with FURA 2 and by confocal microscopy. Determination of Ca^{2+}-ATPase activity was followed by Pi measurements. Changes in the mitochondria electrochemical potential was followed with Rhodamine 123. Apoptosis and DNA fragmentation were determined by TUNEL experiments.
Results Upon agelasine B treatment, cell viability of both human breast cancer cell lines was one order of magnitude lower as compared with fibroblasts (IC_{50} for MCF-7 = 2.99 μM; SKBr3: IC_{50} = 3.22 μM vs. fibroblasts: IC_{50} = 32.91 μM), while the IC_{50} for PC-3 IC_{50} = 6.86 μM. Agelasine B induced a large increase in the intracellular Ca^{2+} concentration in MCF-7, SKBr3, and PC-3 cells. By the use of confocal microscopy coupled to a perfusion system, we could observe that this toxin releases Ca^{2+} from the endoplasmic reticulum (ER). We also demonstrated that agelasine B produces a potent inhibition of the ER Ca^{2+}-ATPase (SERCA), and that this compound induced the fragmentation of DNA. Accordingly, agelasine B reduced the expression of the anti-apoptotic protein Bcl-2 and was able to activate caspase 8, without affecting the activity of caspase 7.
Conclusions Agelasine B in MCF-7 cells induce the activation of apoptosis in response to a sustained increase in the $[Ca^{2+}]_i$ after blocking the SERCA activity. The reproduction of the effects of agelasine B on cell viability and on the $[Ca^{2+}]_I$ obtained on SKBr3 and PC-3 cancer cells strongly suggests the generality of the mechanism of action of this toxin.

Keywords Calcium · Natural products · Agelasine B · Thapsigargin · SERCA

A. A. Pimentel · L. Colman · A. Mayora · M. L. Silva · R. Dipolo · F. Arvelo · I. Galindo-Castro · G. Benaim (✉)
Instituto de Estudios Avanzados (IDEA), Carretera Nacional Hoyo de la Puerta, Sartenejas, Baruta, Caracas, Venezuela
e-mail: gbenaim@idea.gob.ve

A. A. Pimentel · A. I. Suarez
Facultad de Farmacia, Universidad Central de Venezuela (UCV), Caracas, Venezuela

P. Felibertt
Facultad de Ciencias, Universidad de Carabobo, Valencia, Carabobo, Venezuela

F. Sojo · A. Mayora · F. Arvelo · G. Benaim
Instituto de Biología Experimental, Facultad de Ciencias, UCV, Caracas, Venezuela

L. Colman · H. Rojas · R. Dipolo
Instituto Venezolano de Investigaciones Científicas (IVIC), Caracas, Venezuela

R. S. Compagnone
Escuela de Química, Facultad de Ciencias, UCV, Caracas, Venezuela

J. B. De Sanctis · P. Chirino
Instituto de inmunología, UCV, Caracas, Venezuela

Introduction

There is an increasing interest in the development of new drugs derived from natural products for the treatment of

cancer. In this respect, it has been shown that some natural compounds derived from marine sponges possess different cytotoxic activity [1]. In particular, agelasines which are mono- or bi- cyclic diterpenoids having a 9-methyladenine chromophore [1] has been demonstrated to have antimicrobial [2], antimalarial [3], leishmanicidal, trypanocidal [4], and even antileukemic activities [5].

In the present work, we purified agelasine B (Fig. 1a) from the marine sponge *Agelas clathrodes* and studied its relative cytotoxic activity against human breast cancer MCF-7 cells when compared with human fibroblasts. It is well known that different cancer cells evade programmed cell death. On the other hand, apoptosis is directly associated with a transfer of Ca^{2+} from the endoplasmic reticulum (ER) to the mitochondria [6, 7]. The Ca^{2+} concentration in the ER is about fourth order of magnitude higher than the cytoplasmic Ca^{2+} concentration ($[Ca^{2+}]_i$) [8]. This accumulation is due to the action of the sarco(endo)plasmic Ca^{2+}-ATPase (SERCA). Ca^{2+} has been recognized as an important second messenger with a key role in different processes related to cell growth control and differentiation, in addition to apoptosis.

In this work, we studied the effect of agelasine B on $[Ca^{2+}]_i$ regulation, following $[Ca^{2+}]_i$ changes in the cell upon addition of this natural compound, using a confocal microscopy system associated to a rapid perfusion devise. We demonstrated that agelasine B is able to provoke a large increase in the $[Ca^{2+}]_i$, as a consequence of the direct inhibition of the SERCA activity, which in turn induced the release of Ca^{2+} from the endoplasmic reticulum. Thapsigargin (Tg), a well known specific inhibitor of the SERCA, provokes the so-called endoplasmic reticulum stress, sensitizing, and/or promoting many cells to enter in apoptotic program [9–14]. In this work, we demonstrated that, similarly to thapsigargin, agelasine B induces apoptosis onset in human breast cancer MCF-7 cells, as determined by the activation of caspase 8, decreased expression of the anti-apoptotic protein Bcl-2 and DNA fragmentation.

Materials and methods

Marine sponge samples

The marine sponge, *Agelas clathrodes*, was collected at 15 mts deep in the island La Blanquilla, located at 150 miles northwest of Margarita Island, Venezuela. The sponges were washed with sea water, frozen and identified by Prof. Sheila Marques of Escuela de Biologia, Facultad de Ciencias, Universidad Central de Venezuela.

Extraction and purification of agelasine B

Frozen samples (114.7 g) of *Agelas clathrodes* were liophilized and extracted with methanol (MeOH) (2 × 1.5 l). The residue of evaporation of the methanol extract was dissolved in a mixture of MeOH/H_2O (1:1) and partitioned with chloroform. After evaporation of the solvent, the chloroform extract (4.07 g) was passed through a chromatography column of Sephadex LH-20 and eluted with chloroform ($CHCl_3$)/MeOH (1:1) to obtain six fractions (**1**–**6**) with different RFs. Fraction **3** derived from this column was subjected to repeated separation through series of chromatographic columns using $CHCl_3$/MeOH/NH_4OH, changing the ratio from 95:4:1 to 80:19:1 to obtain agelasine B (298 mg) as a yellow powder ($C_{26}H_{40}N_5Cl$), with following analytical parameters: m.p. 168–170°C. [15]. EIMS 459.096, IR 3,379, 3,110, 2,937, 2,873, 1,662, 1,591, 1,200 cm^{-1}, NMR ^1H ($CDCl_3$, 270 MHz) δ 0.73 (3H, s); 0.75 (3H, d, $J = 5.2$ Hz); 1.01–2.1 (14H, m); 1.15 (3H, s); 1.49 (1H, brs); 1.77 (3H, brs); 4.04 (3H, brs); 5.23 (1H, brs); 5.37 (1H, brt, $J = 6.5$ Hz); 5.45 (2H, s); 7.50 (2H, brs, exch), 8.39 (1H,s); 10.34 (1H, s). NMR ^{13}C ($CDCl_3$, 67.5 MHz) δ 15.6 (q); 16.9 (q); 17.6 (q); 17.8 (q); 17.9 (t); 19.5 (q); 26.5 (t); 27.0 (t); 31.6 (q); 32.7 (t); 35.9 (d); 36.0 (t); 36.4 (t); 37.8 (s); 38.3 (s); 46.1(d); 48.3 (t); 109.8 (s); 115.3 (d); 120.5 (d), 141.7 (d); 144.6 (s); 148.1 (s); 149.7 (s); 152.8 (s); 156.3 (d).

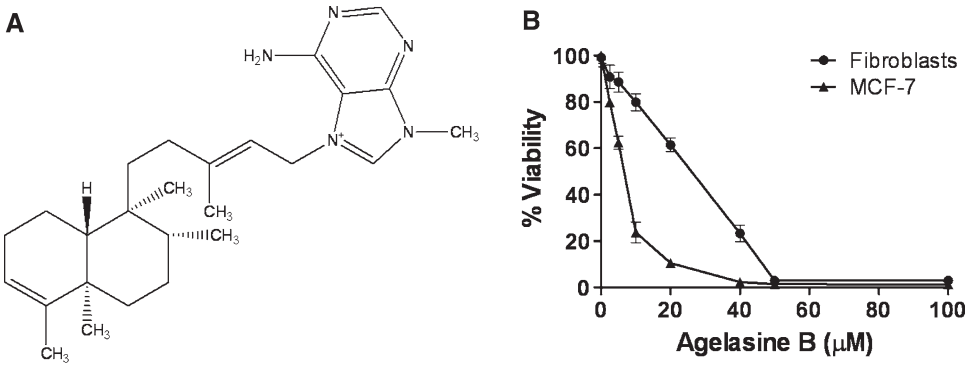

Fig. 1 **a** Chemical structure of agelasine B. **b** Effect of agelasine B on MCF-7 cells and fibroblasts. A dose–response curve of % viability for MCF-7 cells and fibroblast treated with agelasine B (see text for experimental details). Each point represents the mean ± SD of at least 5 independent experiments

Culture cell lines

The human breast cancer cell line MCF-7 was grown in Dubelcco's modified Eagle Medium (DMEM), supplemented with 10% fetal bovine serum (FBS), penicillin (100 U/ml), and streptomycin (10,000 μg/ml). Cells were grown in a humidified incubator with atmosphere of 5% CO_2 and 95% air at 37°C. Human dermis fibroblasts were obtained from primary cultures of tissue explants of normal individuals and maintained in supplemented DMEM as mentioned before. An informed consent document was obtained from the fibroblasts' donors.

Cytotoxicity assays

Cytotoxicity tests were carried out by following the colorimetric reduction of 3-(4,5-dimethylthiazol-2-yl)-2,5-diphenyltetrazolium bromide (MTT) to formazan [16]. Briefly, cells were subcultured into 96-well tissue culture plates containing 5,000 cells per well and reaching confluency after 24 h of culture. At this point, cells were exposed to agelasine B for 48 and 72 h at concentrations ranging from 1 to 100 μM. In all cases, agelasine B was dissolved in dimethylsulfoxide (DMSO). The final concentration of this solvent was equal or lower than 0.5%.

Appropriate controls were performed with 0.5% DMSO. After treatment with agelasine B, the cells were incubated with 0.5 mg/ml MTT for 3 h at 37°C. At the end of the experiment, the supernatant was removed and DMSO (100 μl) was added to dissolve formazan crystals, and absorbance was measured on a multi-detection microplate reader (Synergy HT, Bio-Tek) at 570 nm. The IC_{50} value was defined as the concentration of agelasine B resulting in a 50% reduction of absorbance compared with untreated cells, using the software Graphpad Prism 5.0.

Measurement of Ca^{2+} concentration

Measurement of $[Ca^{2+}]_i$ in MCF-7 cells was performed by the use of the fluorescent indicator Fura-2 as reported previously [19] with some modifications. Briefly, a cell suspension (1.0×10^6 cells/ml) in medium containing 138 mM NaCl, 5 mM KCl, 1 mM $MgCl_2$, 1.5 mM $CaCl_2$, 5 mM glucose, 10 mM HEPES (extracellular medium) and then loaded with 200 μM of sulfinpyrazone, 0.025% pluronic acid, 0.1% BSA, and 3 μM Fura-2-AM, for 30 min at 25°C under constant agitation in darkness. After loading, MCF-7 cells were resuspended and incubated for 15 min in the extracellular medium, and then washed again with the same medium. The fluorescence of Fura-2 in the loaded cell suspension was monitored with a spectrofluorimeter Perkin Elmer LS 55, provided with an acquisition system for excitation ratio measurements with continuous agitation in a stirred cuvette. The excitation wavelengths were set at 340 and 380 nm, and emission was measured at 510 nm. All the experiments were performed at 30°C. Intracellular Ca^{2+} concentration was calculated by the method of Grynkiewicz et al. [19], using the following expression:

$$[Ca^{2+}]_i = K_d[(R - R_{\min})/(R_{\max} - R)]F_{\min(380)}/F_{\max(380)}.$$

where R is F_{340}/F_{380} ratio, $R_{\min}$ and $R_{\max}$ are the ratios at 0 Ca^{2+} (6 μM digitonin plus 4 mM EGTA) and saturating Ca^{2+} (2 mM $CaCl_2$ plus 6 μM digitonin), respectively. *Kd* represents the apparent dissociation constant of Fura-2 (224 nM) and $F_{\min(380)}/F_{\max(380)}$ are the fluorescence values of digitonized cells (6 μM digitonin) plus 4 mM EGTA and 2 mM CaCl2, respectively. Values of $R_{\min}$ and $R_{\max}$ were measured in situ in MCF-7 cells. The same protocol was used for the determination of changes in $[Ca^{2+}]_i$ in SKBr3 cells. In the case of PC-3, the loading of Fura 2 was performed in RPMI supplemented with 5% FCS, in the presence of 2 μM Fura 2-AM for 45 min. at 25°C under constant agitation, and the experiments were performed at 37°C.

Detection of intracellular Ca^{2+} signaling by confocal microscopy

Intracellular Ca^{2+} was monitored in individual cells by using time-scan confocal microscopy [17, 18]. MCF-7 cells were incubated with Rhod-2/AM (10 μM) for 45 min at 37°C in a 22 × 40 mm glass coverslip with 0.01% poly-L-lysine in the culture medium. After incubation, the cells were washed with extracellular medium. Finally, the cells were incubated with BODIPY-FL-Ryanodine (500 nM) for 15 min at 37°C. The coverslip with the dual-loaded cells was attached to an open experimental chamber (RC-27, Warner Instruments, Handem, CT) coupled to a laser scanning confocal microscope (LSCM, Nikon C1), mounted in a Eclipse TE300 Nikon inverted microscope with Nikon 100/1.30 oil Ph4L oil-immersion objective coupled to a C1-LU2 laser unit with neon-(543 nm) and argon-cooled air (488 nm). This laser unit was controlled by a D-eclipse C1 interface. Experiments were performed using a DAD-12 perfusion system with a PTR-2000 perfusion temperature regulator (Adam & List Associates, Westbury, NY) stage to deliver the test solutions to the MCF-7 cells via pressure ejection from a 200 μM ID carbonate pipette. This device allows a computer to control the changes of different experimental solutions as fast as 20 ms (measured by changing the resistance of a microelectrode placed near the tip of the perfusion cannula after perfusion with extracellular medium). The cells were continuously perfused with this medium at 37°C.

Purification of Ca^{2+}-ATPase from the sarcoplasmic reticulum

Vesicles derived from the longitudinal sarcoplasmic reticulum of rabbit hind leg skeletal muscle were prepared as described by Eletr and Inesi [20]. These vesicles are highly enriched in Ca^{2+}-ATPase (about 90%). The final pellet was resuspended in 20 ml of medium containing 10 mM histidine, 30% sucrose, and stored under liquid nitrogen until used. To ensure that the vesicles did not retain any Ca^{2+} in the lumen, the divalent cation ionophore A-23187 (1 μM) was included in the assay medium.

Determination of the SERCA activity

The purified enzyme (2 μg/ml) was incubated at 37°C for 45 min, under continuous agitation, in 250 μl of a buffer containing 100 mM KCl, 20 mM MOPS-Tris (pH 7.0), 1 mM EGTA, 10 mM $MgCl_2$, 4 mM ATP, 1 μM A-23187, and 1.01 mM $CaCl_2$, in order to obtain a free Ca^{2+} concentration of 10 μM of Ca^{2+}, as calculated by an iterative program as described before [21]. The inorganic phosphate determination was carried out according to the colorimetric method of Fiske and Subbarrow [22], modified by the use of ferrous sulfate as reducing agent, as previously described [23].

Determination of the mitochondrial electrochemical potential ($\Delta\Psi$)

These determinations were carried out using the fluorescent dye rhodamine 123 essentially as previously described [24]. Rhodamine-123 is a mitochondrial-specific cationic dye which allows the visualization of the electrochemical potential state of this organelle, since this dye is distributed between the internal and external mitochondrial membrane according to the electrochemical potential. Rhodamine 123 has a maximum excitation peak at 488 and a maximum emission peak at 530 nm. A cell suspension (1×10^6 cells/ml) was resuspended in a medium containing 138 mM NaCl, 5 mM KCl, 1 mM $MgCl_2$, 1.5 mM $CaCl_2$, 5 mM glucose, 10 mM HEPES–KOH, pH 7.4, and loaded with rhodamine 123 (20 μg/ml) for 30 min, at 30°C. All measurements were performed in a HITACHI F-7000 spectrofluorimeter at 30°C with continuous stirring.

Determination of caspase 8 activity

For the determination of the proteolytic activity of caspase 8, we used the Caspase-Glo 8 Kit (Promega, Madison, WI), following the manufacturer′s instructions. This assay provides a luminogenic caspase 8 substrate, containing the recognition cleavage sequence LETD, and aminoluciferin as the luciferase substrate. Cells (5×10^3 per well) were seeded in a 96-well plate and incubated for 24 h at 37°C. Then, after cell incubation under the different treatments, the luminescent signals were determined using a multi-detection microplate reader (Synergy HT, Bio-Tek). Staurosporine (1 μM) and TNF-α (100 nM) were used as apoptosis inducers (positive controls) and 0.5% DMSO as negative controls, respectively.

Determination of caspase 3/7 activity

We also determined the proteolytic activity of caspase 7 with the Caspase-Glo 3/7 Kit (Promega, Madison, WI) following the manufacturer′s instructions. Since MCF-7 cells do not possess caspase 3 [25], the data reported here correspond to the different treatments effect on caspase 7 activity. A 96-wells tissue culture plate was seeded with 5×10^3 cells per well and incubated for 24 h at 37°C. Then, after the cells were exposed to the different treatments for 24 h, they were lysed and finally the luminescence signal was determined using a multi-detection microplate reader (Synergy HT, Bio-Tek). Staurosporine (1 μM) was used as apoptosis inducer (positive controls) and 0.5% DMSO as negative controls, respectively.

Expression of Bcl-2

MCF-7 cells treated with agelasine B for 24 and 48 h were lysed by adding SDS-lysis buffer (50 mM Tris–HCl pH 8, 0.5% SDS, 10 μM antipain, 10 μg/ml leupeptin 0.2 mM PMSF), centrifuged to separate non-soluble material, and then soluble proteins were transferred onto a Hybond-P membrane (Amersham Pharmacia) with the use of a Mini Trans-Blot Electrophoretic transfer cell system (Bio-Rad). The membranes were incubated with a mouse anti-human Bcl-2 antibody (Sigma, MO) or a rabbit anti-GAPDH antibody (Santa Cruz Biotechnology) overnight at 4°C. After washing with PBS containing 0.05% Tween 20, the membrane was incubated with 1:2,000 diluted peroxidase-conjugated goat anti-(mouse IgG) (Sigma, MO) or mouse anti-rabbit (Santa Cruz, Biotechnology) for 1 h at room temperature. After another washing step, peroxidase activity was detected by a chemiluminescence method using luminol (Santa Cruz, Biotechnology) according to the manufacturer's instructions. Proteins were determined by the method of Bradford using bovine serum albumin as a standard.

Determination of nuclear DNA fragmentation

The dead-end fluorimetric TUNEL (TdT-mediated dUTP Nick-End labeling) system Kit (Promega) was used to measure DNA fragmentation. Cells were double-stained with both fluorescein-12-dUTP labeled DNA (which stains

specifically the fragmented DNA) and propidium iodide and analyzed by flow cytometry (Epics XL Beckman Coulter, FL), according to the manufacturer's instructions. Cells without treatment were used as negative controls. The amount of apoptosis and necrosis markers in negative controls were always lower than 5%. Cells treated with 1 μM staurosporine were used as positive controls.

Results

Differential cytotoxic effect of agelasine B on MCF-7 cells and human fibroblasts

We first studied the cytotoxic effect of agelasine B on the human breast cancer cell line MCF-7 as compared with human fibroblasts, by the use of the MTT Assay (Fig. 1b). The results showed that the natural product decreased cell viability in a dose-dependent manner, reaching an IC_{50} of 2.99 μM. This value was about one order of magnitude lower in the cancer cell line than in fibroblasts ($IC_{50} = 32.91$ μM). The IC_{50} values were obtained from the data in Fig. 1b. These results also support the notion that this natural product is more effective in rapidly dividing cells when compared with normal ones. In order to study the possible generality of this effect, we calculated the IC_{50} in other cancer cell lines. First, we used SKBr3, which is also a breast cancer cell line, but differs from MCF-7 since SKBr3 over-expresses the EGFR and lacks classic estrogen receptors. We also studied another unrelated cancer cell line, PC-3, which is an androgen-independent prostate cancer cell line. The results are summarized in Table 1. It can be observed that while the IC_{50} for SKBr3 was similar to MCF-7 ($IC_{50} = 3.22$ μM), the IC_{50} obtained for PC-3 ($IC_{50} = 6.86$ μM) is double than the former. Nevertheless, the values remain at the same order of magnitude, and significantly lower from the IC_{50} found in fibroblasts.

Effect of agelasine B on $[Ca^{2+}]_i$ mobilization in MCF-7 cells

Since Ca^{2+} is involved in many signaling processes related to cell growth, differentiation, and apoptosis, we tested the effect of agelasine B on the resting $[Ca^{2+}]_i$. A cellular suspension of MCF-7 cells was incubated with Fura-2 AM in the presence of extracellular Ca^{2+}, and the $[Ca^{2+}]_i$ was monitored as described under "Materials and methods". As illustrated in Fig. 2, a rapid biphasic increase in the cytoplasmic Ca^{2+} was obtained upon addition of 5 μM agelasine B (Fig. 2a), reaching a peak of about three times the basal level followed by a reduction to a sustained plateau. This attained new level is higher than the initial basal one (Fig. 2a). This result is typical of signals that induce the liberation of Ca^{2+} from the endoplasmic reticulum (ER), with the subsequent activation of plasma membrane Ca^{2+} channel named "store operated Ca^{2+} entry (SOCC), or capacitative Ca^{2+} entry [17, 18]. This effect is very similar to that obtained with the well-known SERCA inhibitor thapsigargin (Tg) (see Fig. 2b). Addition of agelasine B after the treatment with Tg, elicit no effect on the Ca^{2+} concentration (Fig. 2b). Accordingly, the addition of Tg after the sustained plateau induced by agelasine B was not able to increase $[Ca^{2+}]_i$ in an additive form (Fig. 2a). This results support the notion that the action of both compounds generate similar responses.

The opening of a capacitative Ca^{2+} entry was corroborated performing the same experiments in the absence of external Ca^{2+} (Fig. 2c, d). Under these conditions, the peaks reached after agelasine B or Tg addition are significantly lower than that obtained in the presence of external Ca^{2+}. Even more, the final Ca^{2+} level elicited is identical to the previous $[Ca^{2+}]_i$ before the addition of agelasine B or Tg. Again, no additive effect was observed when the effectors were added sequentially in both cases (Fig. 2c, d). When 3,5-bis(trifluoromethyl)pyrazole (BTP-2), a classical inhibitor of the SOCC channels, was used, the effect of agelasine B was similar to that obtained in the absence of extracellular Ca^{2+}, corroborating the contribution of the capacitative calcium entry to the overall response (result not shown).

In order to test if the mechanism of action of agelasine B observed in MCF-7 cells is similar in the other cancer cell lines studied (SKBr3 and PC-3), we made experiments measuring the $[Ca^{2+}]_I$ with the same fluorescent Ca^{2+} probe (Fura 2). It can be observed in Fig. 3 that in both cases agelasine B produced similar results to that obtained with MCF-7 cells. Thus, a rapid increase in the $[Ca^{2+}]_I$ followed by a fast decline to a new higher basal level was obtained upon addition of agelasine B in SKBr3 (Fig. 3a) and in PC-3 (Fig. 3e). In both lines, Tg added after agelasine B produced a negligible effect. Also comparable to MCF-7, there was not a significant effect upon the addition of agelasine B after Tg in both cell lines (Fig. 3b, f).

Similarly to MCF-7, when the experiments were performed in the absence of extracellular Ca^{2+} the increase in the $[Ca^{2+}]_I$ generated by agelasine B was significantly

Table 1 Values of IC_{50} for the cytotoxicity of agelasine B in the different cell lines

Cell lines	IC_{50}
Fibroblasts	32.91 ± 1.8
MCF-7	2.99 ± 1.01
SKBr3	3.22 ± 0.99
PC-3	6.86 ± 1.04

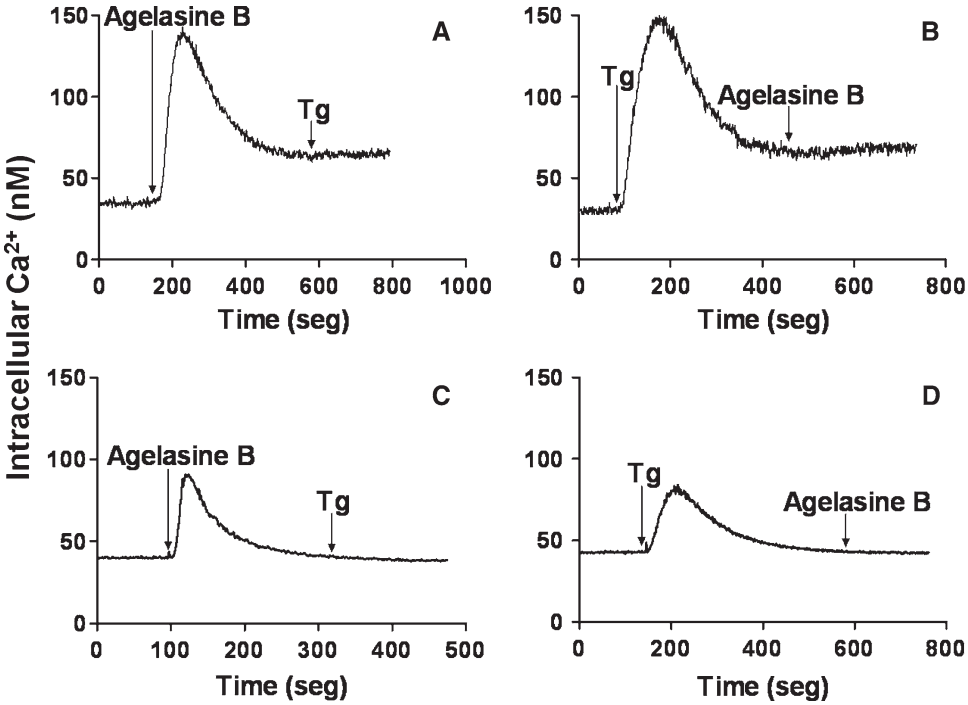

Fig. 2 Effect of agelasine B and thapsigargin (Tg) on the $[Ca^{2+}]_i$ in MCF7. *Arrows* indicate the addition of agelasine B (5 μM) and Tg (1 μM) in the presence of 2 mM $CaCl_2$ (**a** and **b**) and in the absence of $CaCl_2$ (in the presence of EGTA) (**c** and **d**). The *curves* are representative of at least three independent experiments

lower for both cell lines Fig. 3c, g. Accordingly, after addition of Tg, the marine toxin did not induce an extra increase in the $[Ca^{2+}]_I$ (Fig. 3d, h). Taken together, these results support the notion that the mechanism of action of agelasine B is in all these cell lines similar to that of Tg.

Identification of the compartment responsible for Ca^{2+} release induced by agelasine B by confocal microscopy

The intracellular calcium compartment responsible for the release of Ca^{2+} induced by Tg is the ER. In order to identify if agelasine B induces the liberation of Ca^{2+} from this organelle, we used laser scanning confocal microscopy coupled with a microperfussion system adapted to follow rapid changes (milliseconds) in intracellular Ca^{2+} in living single cells [17]. Rhod-2 was used to follow the Ca^{2+} release from the ER, while BODYPY-FL-Ryanodine was used to label the ER (Fig. 4). The red color (Fig. 4a) indicates the level of Ca^{2+} content, while the green color corresponds to the ER (Fig. 4b). The merge of both figures (Fig. 4c) allows the visualization of the region of the ER charged with Ca^{2+} (yellow-orange). The two red organelles observed in red in Fig. 4a, c correspond to the nucleolus, which trapped large quantities of Ca^{2+} [17].

The lower panel represents the same cell, 5 min after addition of agelasine B. It can be observed how the previously wide distribution of Ca^{2+} (red color) associated with the ER disappeared, while the green color corresponding to the ER was not affected. This is depicted in the merged photograph as bleaching of the yellow-orange color (compare Fig. 4c with f). All these results taken together are consistent with our proposal that agelasine B releases Ca^{2+} from the ER.

It can also be noticed in Fig. 4d, f a low but highly disseminated Ca^{2+} signal (red color) in the cytoplasm of the cell, as well as some red spots that probably represent mitochondria, which are known to accumulate Ca^{2+} after its release from the ER [7].

Effect of agelasine B on the SERCA activity

In view of the powerful effect of agelasine B on the liberation of Ca^{2+} from the ER and the lack of thapsigargin effect when added after agelasine B, we investigated the possible effect of this cytotoxic compound on the activity of the SERCA. The Ca^{2+}-ATPase activity was evaluated in the presence or absence of optimal Ca^{2+} concentrations (Fig. 5a, b). Ethanol was used to rule out the presence of a possible contamination of the plasma membrane Ca^{2+}-ATPase, as the latter is known to be largely stimulated by this compound [23]. Ethanol has no effect on the SERCA activity.

As can be observed in Fig. 5, agelasine B indeed inhibits the Ca^{2+}-ATPase activity, at similar levels to that produced by thapsigargin and cyclopiazonic acid, two well-known SERCA inhibitors. This significant inhibitory effect of agelasine B on the SERCA activity occurred in a dose-dependent manner, as can be seen in Fig. 5b. The calculated IC_{50} was 5.58 μM, similar to that obtained for the inhibition of the MCF-7 cell proliferation (Fig. 1b) by agelasine B (2.99 μM).

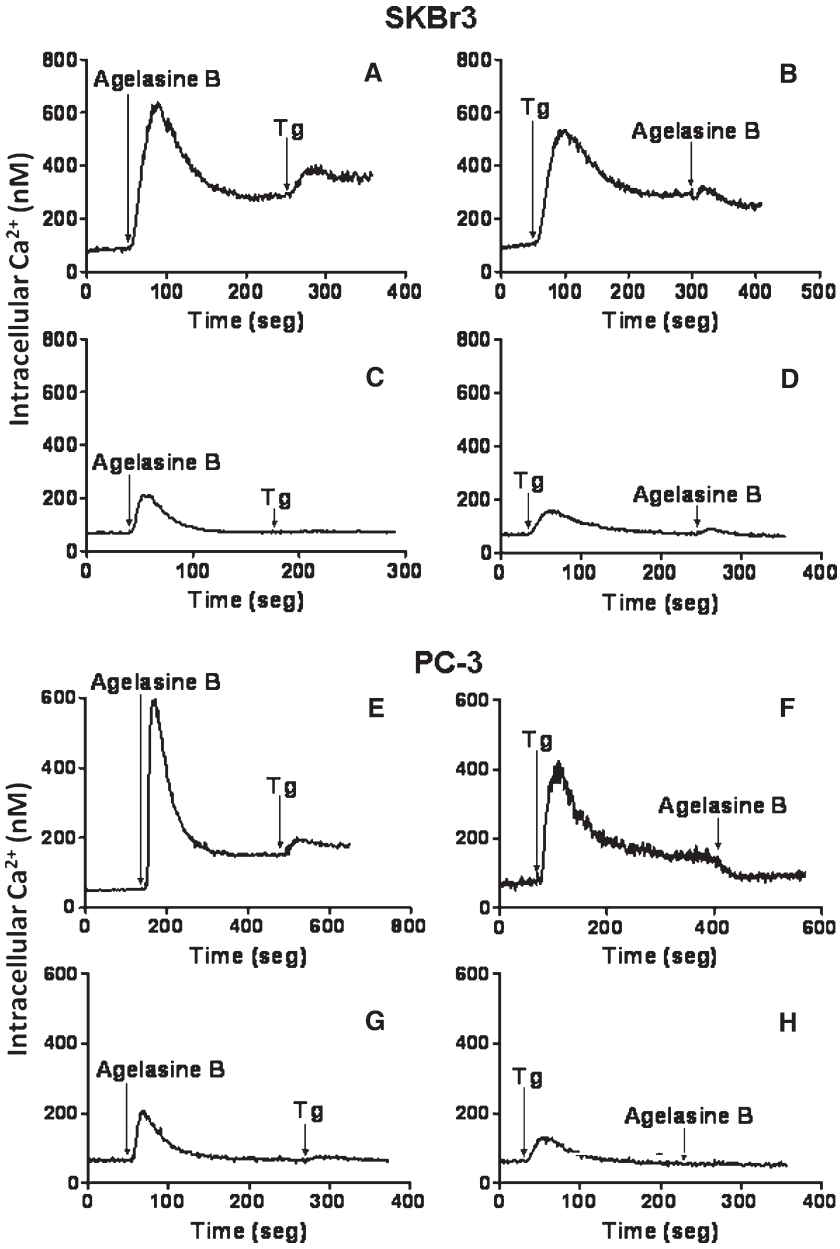

Fig. 3 Effect of agelasine B and thapsigargin (Tg) on the $[Ca^{2+}]_i$ in SKBr3 and PC-3 cells. *Upper panel* (**a**–**d**): SKBr3 cells; *lower panel* (**e**–**h**): PC-3 cells. *Arrows* indicate the addition of agelasine B (5 μM) and Tg (1 μM) in the presence of 2 mM $CaCl_2$ (**a**, **b**, **e**, **f**) and in the absence of $CaCl_2$ (in the presence of EGTA) (**c**, **d**, **g**, **h**). The *curves* are representative of at least three independent experiments

Effect of agelasine B on the electrochemical mitochondrial potential in MCF-7 cells

It is well known that mitochondria accumulate part of the Ca^{2+} just released from the ER [7]. The driving force for this Ca^{2+} transport toward the mitochondrial matrix is the electrochemical gradient caused by the translocation of H^+ that occurs at the internal mitochondrial membrane [26]. Ca^{2+} uptake by mitochondria takes place through an electrophoretic uniport, in such a way that the Ca^{2+} entry gradually dissipates the electrochemical potential ($\Delta\Psi$) [26]. Taking these facts in consideration, we studied the effect of agelasine B and Tg on the electrochemical mitochondrial potential by the use of rhodamine 123, a fluorescent compound that accumulates in the mitochondria depending of the magnitude of the electrochemical potential. The results show that Tg produced a slow but sustained increment in fluorescence due to the liberation of rhodamine 123 (Fig. 5c). This is compatible with the mentioned notion that Tg is able to provoke a partial dissipation of the mitochondrial H^+ gradient, induced by the entry of Ca^{2+}, just released from the ER. Surprisingly, when agelasine B is added after Tg, a further and more pronounced increase in the fluorescence was observed, indicating that this toxin further dissipates the $\Delta\Psi$. This interpretation is corroborated in the experiment shown in Fig. 5d, when agelasine B is added before Tg. It can be seen that the toxin produces a larger increase in

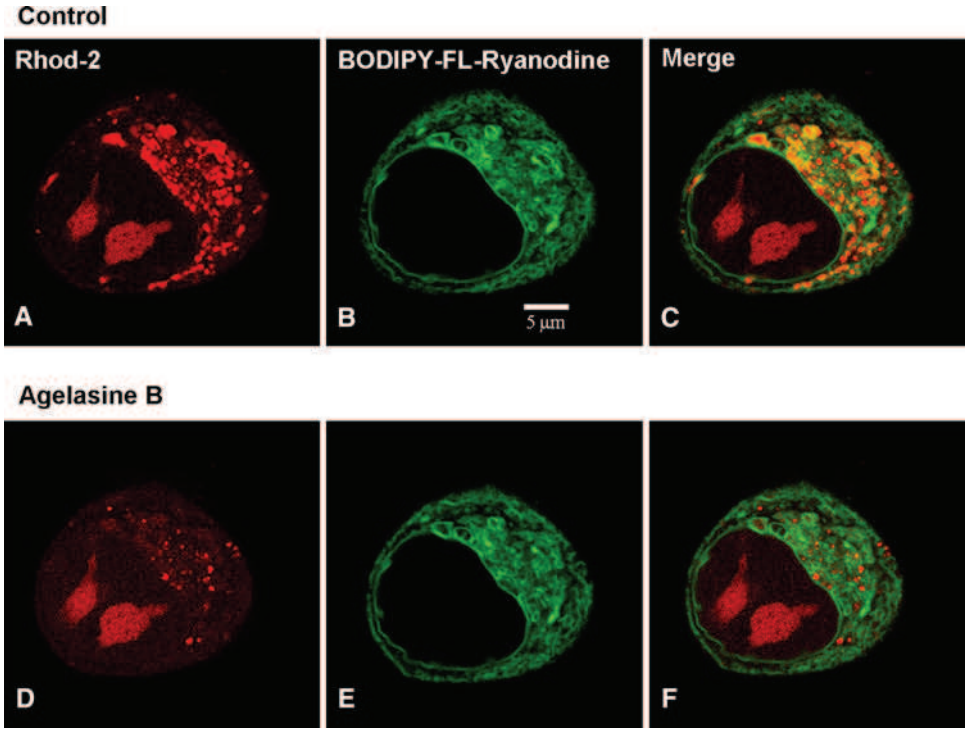

Fig. 4 Identification of the subcellular localization of the sensitive Ca^{2+} pool to agelasine B in MCF-7 cells by confocal microscopy. Cells were incubated with Rhod-2 AM and BODIPY-FL-Ryanodine. *Upper panel* (**a**–**c**): MCF-7 cells in basal conditions; *Lower panel* (**d**–**f**): MCF-7 cells after addition of 10 μM agelasine B. The experiment was performed in the presence of 1 mM $CaCl_2$. The *images* are representative of at least three independent experiments

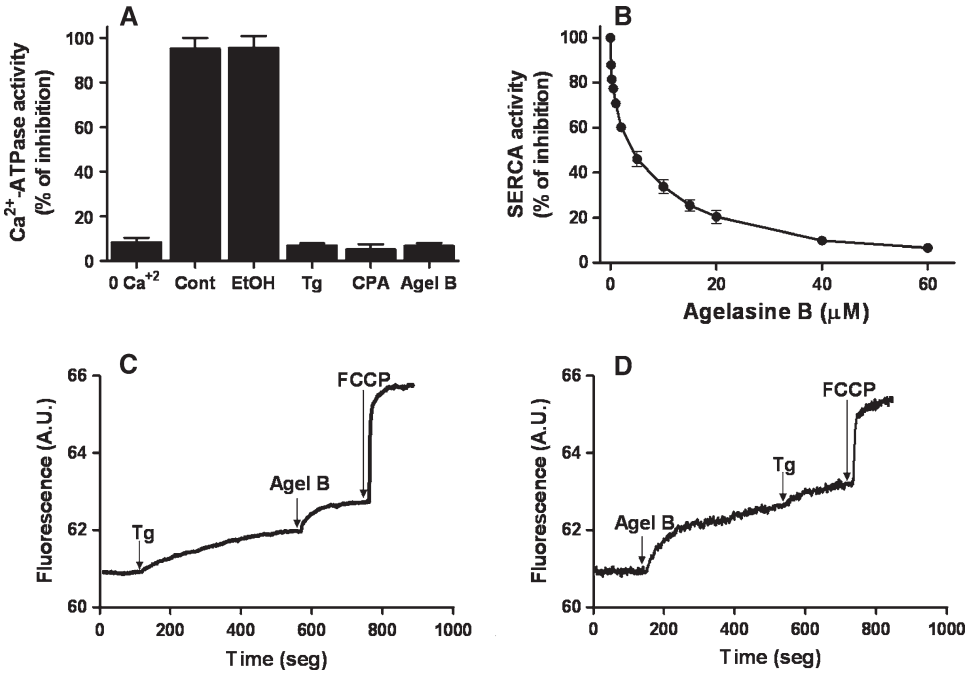

Fig. 5 **a** Effect of agelasine B on the endo(sarco)plasmic reticulum Ca^{2+}-ATPase (SERCA) activity. 0 Ca^{2+}: in the presence of EGTA (1 mM); EtOH: ethanol (5%); Tg: thapsigargin (1 μM); CPA: cyclopiazonic acid (5 μM); Agel B: agelasine B (40 μM). The *bars* represent the mean ± SD of at least 5 independent experiments. **b** Effect of increasing concentrations of agelasine B on the SERCA activity. Each point represents the mean ± SD of at least 5 independent experiments. SERCA vesicles were isolated from rabbit muscle and the Ca^{2+}-ATPase activity was determined as described under "Materials and methods". (**c** and **d**) Effect of agelasine B on MCF-7 cells mitochondrial electrochemical potential. A cell suspension (1×10^6 cells/ml) was loaded with rhodamine 123, as described under "Materials and methods". Fluorescence of rhodamine 123 was followed using an excitation of 488 and emission of 530 nm, under continuous stirring at 30°C. *Arrows* indicate the addition of Tg: thapsigargin (1 μM); Agel B: agelasine B (5 μM); FCCP, (1 μM). The result is representative of at least tree independent experiment

fluorescence when compared with the effect of Tg alone. Accordingly, the effect of Tg after agelasine B is less pronounced. When the protonophore FCCP was added as a positive control, a complete collapse of the electrochemical gradient was observed.

Effect of agelasine B on caspase 8 activity

In order to determine the mechanism by which agelasine B induces cell death in MCF-7 cells, we evaluated the effect of the toxin on the activation of caspase 8, an initiator caspase of apoptosis, in MCF-7 cells. As can be observed in Fig. 6a, the treatment of the cells for 3 h with agelasine B (5 μM) induced a significant increase in caspase 8 activity, similar to the effect induced by the tumoral necrosis factor alpha (TNF-α), which is known to induce that activation of caspase 8, after binding to its receptor. [27]. As expected, staurosporine, albeit been a classical inductor of apoptosis did not modify the activity of caspase 8 (Fig. 6a), since the activation of this caspase by staurosporine depends on the activation of caspase 3 [28], which is absent in MCF-7 cells [25]. We also studied the effect of agelasine B on the activity of caspase 7, one effector caspase of apoptosis. The treatment of MCF-7 cells for 24 h with agelasine B (10 μM) was not able to modify the activity of this caspase with respect to the control (result not shown).

Effect of agelasine B on the expression of the antiapoptotic protein Bcl-2

As a next stept, we evaluated by Western blotting analysis the effect of agelasine B on the expression of the antiapoptotic protein Bcl-2 in MCF-7 cells. After incubation with agelasine B for 48 h, a significant reduction of the expression of Bcl-2 was observed. Staurosporine, an apoptosis inducer through Protein Kinase C inhibition, did not affect the expression of this protein under these experimental conditions (Fig. 6b). As can be seen in the lower panel of Fig. 6b, GAPDH blots showed similar protein loads in each experiment. At 24 h of incubation neither agelasine B nor staurosporine showed any effect on the expression of Bcl-2 (not shown).

Effect of agelasine B on DNA fragmentation in MCF-7 cells

When cells become apoptotic, generally, their nuclei collapse due to an extensive damage to chromatin. DNA-cleavage into regularly spaced oligonucleosomal DNA fragments after selective activation of endogenous endonucleases is commonly observed [29, 30].

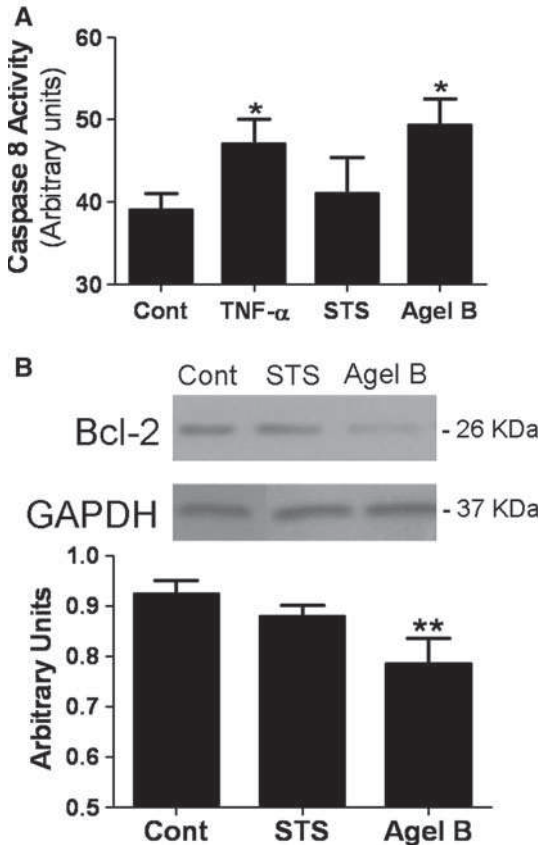

Fig. 6 **a** Effect of agelasine B on caspase 8 activity. Caspase activity was determined as described under "Materials and methods". **b** Effect of agelasine B on Bcl-2 expression. *Upper panel* shows a representative Western blot experiment where anti-Bcl-2 antibody was used to determine the expression levels of the anti-apoptotic protein, after incubation of MCF-7 cells with staurosporine or agelasine B for 48 h. Glyceraldehyde-3-phosphate dehydrogenase (GAPDH) was used as a protein loading control for the Western blots. *Lower panel* Densitometric analysis of the Western blot. *Cont* Control, *TNF-α* tumor necrosis factor α (100 nM), *STS* staurosporine (1 μM), *Agel B* agelasine B (5 μM). The *bars* represent the mean ± SD of at least 3 independent experiments. *($P \leq 0.05$) and **($P \leq 0.01$)

We determined the effect of agelasine B on DNA fragmentation by TUNEL, using staurosporine as positive control and comparing its effect with Tg. Fig. 7a illustrates a typical flow cytometry result in which the effects on cell necrosis (propidium iodide, PI), early apoptosis (TdT), late apoptosis (TdT plus PI), and living cells were recorded by fluorescence intensity. It can be observed that treatment with agelasine B and staurosporine markedly induced apoptosis (early and late) but not necrosis. In this experiment, we also included Tg, showing that with this SERCA inhibitor the pattern remains the same as with agelasine B or staurosporine, further supporting that agelasine B and Tg share, at least in part, the same mechanism of action.

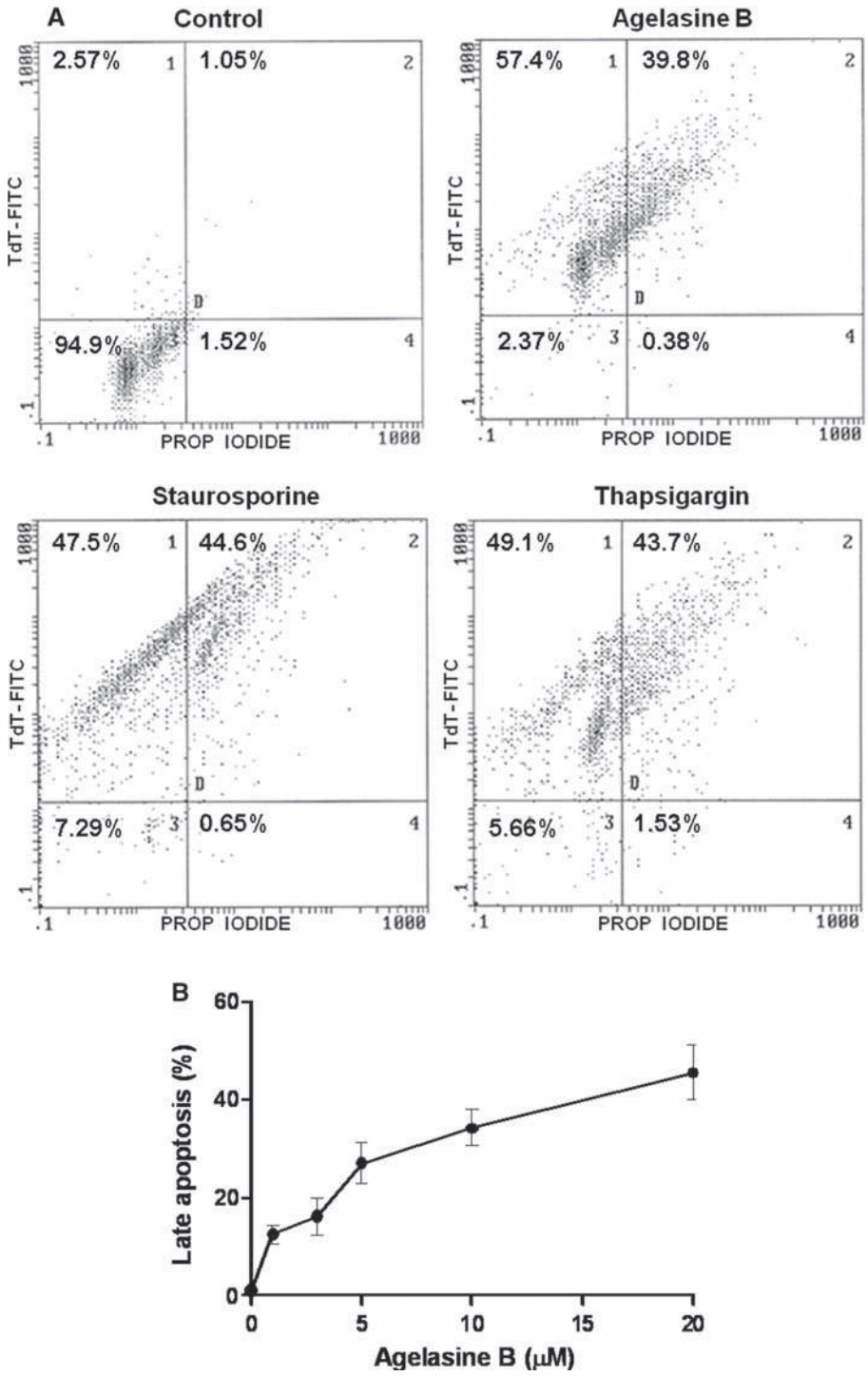

Fig. 7 Effect of agelasine B on nuclear DNA fragmentation. **a** Flow cytometric analysis of flurescein-12-UTP positive MCF-7 cells. Cells were treated with 10 μM agelasine B, 1 μM staurosporine, or 1 μM thapsigargin. Percentages of living cells, flurescein-12-UTP negative-propidium iodide negative (*bottom-zone 3*). Percentages of early apoptotic cells, flurescein-12-UTP positive-propidium iodide negative cells (*top-zone 1*). Percentages of late apoptotic cells, flurescein-12-UTP positive-propidium iodide positive cells (*top-zone 2*). Percentages of necrotic cells, flurescein-12-UTP negative-propidium iodide positive cells (*bottom-zone 4*). The figures show a representative (from three independent) experiment. **b** Effect of agelasine B on the late apoptosis of MCF-7. Different points were obtained from the TUNEL experiments taking the mean of the data from zone 2 of Fig. 6a, which represents the late apoptosis. *Each point* represents the mean ± SD of al least 3 independent experiments

The mean values obtained for the combined early and late apoptosis were 44.8 ± 2.6 for staurosporine, 40.9 ± 2.6 for Tg, and 45.6 ± 5.5 for agelasine B (20 μM), clearly positives for apoptosis, when compared with 1.1 ± 0.2 obtained in the control experiment. The curve showing the effect of agelasine B on the late apoptosis is depicted in Fig. 7b, where a clear dose–response behavior was obtained.

Discussion

It has been demonstrated that some natural compounds of marine origin possess biological and pharmacological activities of potential importance on the search for new drugs against cancer. In this work, we evaluated the effect of agelasine B, a natural diterpene, isolated from the marine sponge *Agelas clathrodes*, on the human breast

cancer MCF-7 cells. The first observation obtained during this work was that agelasine B induced cytotoxity in MCF-7 cells with, at least one order of magnitude, higher potency than in normal (human fibroblasts) cells. In search for the mechanism of action of this toxin, we evaluated its effect on intracellular Ca^{2+} homeostasis. We also observed that the IC_{50} obtained for the cytotoxic effect of agelasine B in MCF-7 cells was reproduced in SKBr3, another breast cancer cell line but which do not possesses classical estrogen receptors and over-expresses EGFR. The IC_{50} obtained in the classical prostate cancer cell line PC-3 was about twice that found in both breast cancer cells. Nevertheless, it was not surprising since it has been reported that the androgen-independent prostate cancer cell lines, as PC-3, are more reluctant to respond to treatments involving Intracellular Ca^{2+} increases (i.e., thapsigargin) driving to apoptosis [31]. However, the IC_{50} for PC-3 was 6,86 μM, which is still significantly lower when compared with fibroblasts ($IC_{50} = 32.91$ μM). Taken together, these results strongly suggest that the effect of agelasine B could be generalized to other cancer cell lines.

The results obtained in suspensions of MCF-7 cells demonstrated that agelasine B is able to induce a fast Ca^{2+} release from an intracellular compartment. Hence, after reaching a peak, the $[Ca^{2+}]_i$ returns to a level which is higher than the initial Ca^{2+} concentration. This is consistent with the release of Ca^{2+} from the endoplasmic reticulum, which in turn induces the opening of a capacitative Ca^{2+} entry (SOCC) through the plasma membrane. These results are similar to that induced by Tg, the classical inhibitor of the SERCA. Even more, the effect of agelasine B was not additive to that of Tg, suggesting the same mechanism of action. The same general pattern was obtained when agelasine B was used on SKBr3 and PC-3 cells, strongly supporting the same mechanism of action of this toxin for the elevation of the $[Ca^{2+}]_i$.

The corroboration that the endoplasmic reticulum was in fact the source of Ca^{2+} release was assessed in isolated cells by means of a confocal microscope system coupled to a fast perfusion device for measuring rapid changes in the extracellular milieu. These results clearly demonstrate that agelasine B indeed produces a rapid release of Ca^{2+} from the ER.

We then studied the mechanism of action of agelasine B on this organelle, focusing on the possibility that this toxin, similar to Tg, could affect the SERCA activity. The results demonstrated that this was certainly the case, since a clear inhibition of this Ca^{2+}-ATPase was observed upon addition of agelasine B in a dose-dependent manner. It is interesting to notice that the calculated IC_{50} for this inhibition was very similar to that obtained in the experiments that showed the cytotoxiticy of agelasine B in MCF-7 (compare Fig. 1b with 5b), further supporting the notion that these two compounds share, at least partially, the same mechanism of action. In this context, it is worth to mention that agelasine B also inhibits the Na^+/K^+-ATPase [32]. This Na^+ pump also belongs to the family of the so called "P" type ATPases [33].

It is well known that mitochondrial Ca^{2+} accumulation is a prerequisite for the final decision in the establishment of cell apoptosis [7, 34]. The main source of mitochondrial Ca^{2+} is its transfer from the ER. Therefore, Ca^{2+} concentration in the ER modulates the magnitude of ion transfer to the mitochondria, and hence, the onset of apoptosis [6, 34]. On this perspective, the results obtained during this work concerning the large effect of agelasine B on the Ca^{2+} content on the ER bring us to study the effect of this compound and Tg on the mitochondrial electrochemical potential, since this gradient represents the driving force for Ca^{2+} accumulation in these organelles. The results show that Tg was able to induce the partial dissipation of the mitochondrial H^+ gradient, as can be seen by the increment in fluorescence due to the liberation of rhodamine 123. This was expected since a large supply of Ca^{2+} to the mitochondria from the ER drives the accumulation of this cation in theses organelles [7, 18]. Therefore, these results demonstrated that, besides the effect of Tg, agelasine B produced a further dissipation of this gradient that cannot be solely explained by the larger supply of calcium around the mitochondria released from the ER. Thus, agelasine B appears to directly affect the mitochondrial electrochemical potential and would imply that this toxin should produce further functional effects on MCF-7 cells, when compared with Tg.

Since the lost of the mitochondrial membrane potential is a characteristic feature of apoptosis, we decided to study the effect of agelasine B on classical proteins associated with the onset of the programmed cell death. Among these proteins, several caspases are activated in a strict order in the cell committed to die. Our results demonstrated that agelasine B was able to increase the activity of caspase 8 to the same level attained by TNFα, known to act through the extrinsic route, upon the binding to the dead receptor specific for this factor [27]. This was interesting since it has been reported that Tg does not induce activation of caspase 8, at least in MCF-7 cells [35]. Hence, albeit agelasine B shares part of the mechanism of action of Tg concerning the inhibition of SERCA activity, its extra effect on the mitochondrial electrochemical potential demonstrated during this work suggest that agelasine B could be affecting proapoptotic proteins in a different way Tg does. It is also conceivable that this toxin produces in these cells other effect besides the two founded during this work.

Other evidence that suggests a direct action of agelasine B in the onset of apoptosis was the significant lowering of Bcl-2 expression obtained upon addition of the toxin. In

these experiments, staurosporine failed to modify the expression of this antiapoptotic protein, even after 48 h of incubation. This was not unexpected, since it has been reported that staurosporine was not able to affect the expression of Bcl-2 in MCF-7 cells, when incubated between 3 and 24 h [36].

We also demonstrated that agelasine B induces DNA fragmentation, as visualized by TUNEL experiments. The effect was dose-dependent and similar to those obtained with Tg and staurosporine.

Taken together, our results indicate that although agelasine B does not share all the action mechanisms of staurosporine and Tg, the final effect is similar since these toxins induce fragmentation of nuclear DNA, one hallmark of the late stage of apoptosis.

It have been demonstrated that thapsigargin is able to induce ER stress which in turn drives to apoptosis [9–11, 13, 14]. The ER is the site of synthesis, folding, and maturation of many proteins. Under ER stress conditions, a reduction of the ER protein folding capacity take place, resulting in the accumulation of unfolded proteins. These unfolded proteins are toxic to the cell and if the homeostatic mechanisms that recover the normal function of the ER fail, the cell can become apoptotic [37, 38]. The effect of thapsigargin has been attributed to the ability of this compound to induce the release of Ca^{2+} from the ER, disrupting the homeostasis of this organelle [9, 14].

In this context, it has been reported the possible use of Tg as prodrug in the treatment of metastatic prostate cancer PC-3 cells, rising the possibility of its potential therapeutic use [12, 14, 39, 40]. Since agelasine B shares with Tg its ability to inhibit the SERCA activity and hence the release of Ca^{2+} from the ER, it could be considered for the rational development of new anticancer drugs.

Acknowledgments This work was supported by grants from Fondo Nacional de Ciencia, Tecnologia e Investigación Venezuela (FONACIT) (G-2001000637), and from the Consejo de Desarrollo Científico y Humanístico (C.D.C.H.-U.C.V.), Universidad Central de Venezuela (PI 03-00-7380-2008/2) to G.B. A.A.P. and A.M. were supported by a graduate student fellowship program from the FONACIT, Venezuela.

Conflict of interest The authors declare that there is not Conflict of Interest concerning this manuscript.

References

1. Gordaliza M (2009) Terpenyl-Purines from the sea. Mar Drugs 7:833–849
2. Vik A, Hedner E, Charnock C, Tangen LW, Samuelsen O, Larsson R, Bohlin L, Gundersen LL (2007) Antimicrobial and cytotoxic activity of agelasine and agelasimine analogs. Bioorg Med Chem 15:4016–4037
3. Gademann K, Kobylinska J (2009) Antimalarial natural products of marine and freshwater origin. Chem Rec 9:187–198
4. Vik A, Proszenyak A, Vermeersch M, Cos P, Maes L, Gundersen LL (2009) Screening of agelasine D and analogs for inhibitory activity against pathogenic protozoa; identification of hits for visceral leishmaniasis and chagas disease. Molecules 14:279–288
5. Ishida K, Ishibashi M, Shigemori H, Sasaki T, Kobayashi J (1992) Agelasine G, a new antileukemic alkaloid from the Okinawan marine sponge Agelas sp. Chem Pharm Bull 40:766–767
6. Scorrano L, Oakes SA, Opferman JT, Cheng EH, Sorcinalli MD, Pozzan T, Korsmeyer SJ (2003) BAX and BAK regulation of endoplasmic reticulum Ca^{+2}: a control point of apoptosis. Science 300:135–139
7. Pinton P, Ferrari D, Magalhaes P, Schulze-Osthoff K, Di Virgilio F, Pozzan T, Rizzuto R (2000) Reduced loading of intracellular $Ca(^{2+})$ stores and downregulation of capacitative $Ca(^{2+})$ influx in Bcl-2-overexpressing cells. J Cell Biol 148:857–862
8. Carafoli E (1987) Intracellular calcium homeostasis. Annun Rev Biochem 56:395–433
9. Jackisch C, Hahm HA, Tombal B, McCloskey D, Butash K, Davidson NE, Denmeade SR (2000) Delayed micromolar elevation in intracellular calcium precedes induction of apoptosis in thapsigargin-treated breast cancer cells. Clin Can Res 6:2844–2850
10. Lei P, Abdelrahim M, Cho SD, Liu S, Chintharlapalli S, Safe S (2008) 1, 1-Bis(3'-indolyl)-1-(p-substituted phenyl)methanes colon cancer cell and tumor growth through activation of c-jun N-terminal kinase. Carcinogenesis 29:1139–1147
11. Chen LH, Jiang C, Watts R, Thorne RF, Kiejda KA, Zhang XD, Hersey P (2008) Inhibition of endoplasmic reticulum stress–induced apoptosis of melanoma cells by the ARC protein. Cancer Res 68:834–842
12. Denmeade SR, Jakobsen CM, Janssen S, Khan SR, Garrett E, Lilja H, Christensen SB, Isaacs JT (2003) Prostate-specific antigen-activated thapsigargin prodrug as targeted therapy for prostate cancer. J Natl Cancer Inst 95:990–1000
13. Sun S, Han J, Ralph WM Jr, Chandrasekaran A, Liu K, Auborn KJ, Carter TH (2004) Endoplasmic reticulum stress as a correlate of cytotoxicity in human tumor cells exposed to diindolylmethane in vitro. Cell Stress Chaperones 9:76–87
14. Wu Y, Fabritius M, Ip C (2009) Chemotherapeutic sensitization by endoplasmic reticulum stress: increasing the efficacy of taxane against prostate cancer. Cancer Biol Ther 8:146–152
15. Wu H, Nakamura H, Kobayashi J, Kobayashi M, Ohizumi Y, Hirata Y (1986) Structure of agelasines, diterpenes having a 9-methyladeninium chromophore isolated from the okinawan marine spomge agelas nakamurai hoshino. Bull Chem Soc Jpn 59:2495–2504
16. Mosman T (1983) Rapid colorimetric assay for cellular growth and survival: application to proliferation and cytotoxicity assays. J Immunol Methods 65:55–63
17. Colina C, Flores A, Rojas H, Acosta A, Castillo C, Garrido MR, Israel A, DiPolo R, Benaim G (2005) Ceramide increase cytoplasmic Ca^{2+} concentration in Jurkat T cells by liberation of calcium from intracellular stores and activation of a store-operated calcium channel. Arch Biochem Biophys 436:333–345
18. Colina C, Flores A, Castillo C, Garrido MR, Israel A, DiPolo R, Benaim G (2005) Ceramide-1-P induces Ca2+ mobilization in Jurkat T-cells by elevation of Ins(1, 4, 5)-P3 and activation of a store-operated calcium channel. Biochem Biophys Res Commun 336:54–60
19. Grynkiewicz G, Poenie M, Tsien RY (1985) A new generation of Ca^{2+} indicators with greatly improved fluorescence properties. J Biol Chem 260:3440–3450

20. Eletr S, Inesi G (1972) Phospholipid orientation in sarcoplasmic membranas: spin-label ESR and proton NMR studies. Biochim Biophys Acta 282:174–179
21. Suju M, Davila M, Poleo G, Docampo R, Benaim G (1996) Phosphatidylethanol stimulates the plasma-membrane calcium pump from human erythrocytes. Biochem J 317:933–938
22. Fiske CH, SubbaRow Y (1925) The colorimetric determination of phosphorus. J Biol Chem 66:375–400
23. Benaim G, Cervino V, Lopez-Estraño C, Weitzman C (1994) Ethanol stimulates the plasma membrane calcium pump from human erythrocytes. Biochim Biophys Acta 1195:141–148
24. Benaim G, Sanders JM, García-Marchan Y, Colina C, Lira R, Caldera AR, Payares G, Sanoja C, Burgos JM, Leon-Rossell A, Concepcion JL, Schijman AG, Levin M, Oldfield E, Urbina JA (2006) Amiodarone has intrinsic anti-Trypanosoma cruzi activity and acts synergistically with posaconasol. J Med Chem 49:892–899
25. Kagawa S, Gu J, Honda T, McDonnell TJ, Swisher SG, Roth JA, Fang B (2001) Deficiency of caspase-3 in MCF7 cells blocks Bax-mediated nuclear fragmentation but not for cell death. Clin Cancer Res 7:1474–1480
26. Benaim G, Bermúdez R, Urbina J (1990) Ca^{2+} transport in isolated mitochondrial vesicles from Leishmania braziliensis promastigotes. Mol Biochem Parasitol 39:61–68
27. Grupta S (2002) Decision between life and death during TNF-induced signaling. J Clin Immunol 22:270–278
28. Tang D, Lahti JM, Kidd VJ (2000) Caspase-8 activation and bid cleavage contribute to MCF7 cellular execution in a caspase-3-dependent manner during staurosporine-mediated apoptosis. J Biol Chem 275:9303–9307
29. Schwartzman RA, Cidlowski JA (1993) Apoptosis: the biochemistry and molecular biology of programmed cell death. Endocrine Rev 14:133–151
30. Bortner CD, Oldenburg NB, Cidlowski JA (1995) The role of DNA fragmentation in apoptosis. Trends Cell Biol 5:21–26
31. Prevarskaya N, Skryma R, Shuba Y (2004) Ca^{2+} homeostasis in apoptotic resistance of prostate cancer cells. Biochem Biophys Res Commun 322:1326–1335
32. Kobayashi M, Nakamura H, Wu HM, Kobayashi J, Ohizumi Y (1987) Mode of inhibition of brain sodium-potassium ATPase by agelasidines and agelasines from a sea sponge. Arch Biochem Biophys 259:179–184
33. Pedersen P, Carafoli E (1987) Ion ATPases, Ubiquity, properties and significance to cell function. Trends Biochem Sci 12:146–150
34. Demaurex N, Distelhorst C (2003) Apoptosis-the calcium connection. Science 300:65–67
35. Fiebig AA, Zhu W, Hollerbach C, Leber B, Andrews DW (2006) Bcl-XL is qualitatively different from and ten times more effective than Bcl-2 when expressed in a breast cancer cell line. BMC Cancer 6:6–213
36. Mooney LM, Al-Sakkaf KA, Brown BL, Dobson PR (2002) Apoptotic mechanisms in T47D and MCF-7 human breast cancer cells. Br J Cancer 87:909–917
37. Rao RV, Ellerby HM, Bredesen DE (2004) Coupling endoplasmic reticulum stress to the cell death program. Cell Death Differ 11:372–380
38. Rasheva VI, Domingos PM (2009) Cellular responses to endoplasmic reticulum stress and apoptosis. Apoptosis 14:996–1007
39. Christensen SB, Skytte DM, Denmeade SR, Dionne C, Møller JV, Nissen P, Isaacs JT (2009) A Trojan horse in drug development: targeting of thapsigargins towards prostate cancer cells. Anticancer Agents Med Chem 9:276–294
40. Vandecaetsbeek I, Christensen SB, Liu H, Van Veldhoven PP, Waelkens E, Eggermont J, Raeymaekers L, Møller JV, Nissen P, Wuytack F, Vangheluwe P (2011) Thapsigargin affinity purification of intracellular P(2A)-type Ca(2+) ATPases. Biochim Biophys Acta 1813:1118–1127